

A lower bound on the maximum mass if the secondary in GW190814 was once a rapidly spinning neutron star

Elias R. Most¹, L. Jens Papenfort¹, Lukas R. Weih¹, Luciano Rezzolla^{1,2,3}

¹ *Institut für Theoretische Physik, Goethe Universität, Max-von-Laue-Str. 1, 60438 Frankfurt am Main, Germany*

² *School of Mathematics, Trinity College, Dublin 2, Ireland*

³ *Helmholtz Research Academy Hesse for FAIR, Max-von-Laue-Str. 12, 60438 Frankfurt am Main, Germany*

Accepted XXX. Received YYY; in original form ZZZ

ABSTRACT

The recent detection of GW190814 featured the merger of a binary with a primary having a mass of $\sim 23 M_{\odot}$ and a secondary with a mass of $\sim 2.6 M_{\odot}$. While the primary was most likely a black hole, the secondary could be interpreted as either the lightest black hole or the most massive neutron star ever observed, but also as the indication of a novel class of exotic compact objects. We here argue that although the secondary in GW190814 is most likely a black hole at merger, it needs not be an ab-initio black hole nor an exotic object. Rather, based on our current understanding of the nuclear-matter equation of state, it can be a rapidly rotating neutron star that collapsed to a rotating black hole at some point before merger. Using universal relations connecting the masses and spins of uniformly rotating neutron stars, we estimate the spin, $0.49_{-0.05}^{+0.08} \lesssim \chi \lesssim 0.68_{-0.05}^{+0.11}$, of the secondary – a quantity not constrained so far by the detection – and a novel strict lower bound on the maximum mass, $M_{\text{TOV}} > 2.08_{-0.04}^{+0.04} M_{\odot}$ and an optimal bound of $M_{\text{TOV}} > 2.15_{-0.04}^{+0.04} M_{\odot}$, of nonrotating neutron stars, consistent with recent observations of a very massive pulsar. The new lower bound also remains valid even in the less likely scenario in which the secondary neutron star never collapsed to a black hole.

Key words: transients: black hole - neutron star mergers — gravitational waves — stars: neutron

1 INTRODUCTION

With the detection of gravitational waves (GW) from a binary black hole (BBH) merger GW190412 (The LIGO Scientific Collaboration & the Virgo Collaboration 2020) with mass ratio of $q = 0.28_{-0.06}^{+0.13}$ by the LIGO/Virgo collaboration, it has been shown that even for more massive BBH a significant mass ratio can be acquired. While the lower mass companion with a mass of $m_2 = 8.4_{-1.0}^{+1.8} M_{\odot}$ is definitely a black hole (BH) in this case, it gave an interesting prospect for the possibility of even more asymmetric binary mergers in the future.

The most recent detection GW190814 (The LIGO Scientific Collaboration et al. 2020) belongs to a binary merger featuring a much lower mass ratio of $q = 0.112_{-0.009}^{+0.008}$ with a massive primary companion of $m_1 = 23.2_{-1.0}^{+1.1} M_{\odot}$ and a secondary of $m_2 = 2.59_{-0.09}^{+0.08} M_{\odot}$, which falls in the possible mass gap between neutron stars (NSs) and stellar BHs. Being the source of the most asymmetric binary compact object merger to date GW190814 seems to challenge the established binary formation channels. It is argued in The LIGO Scientific Collaboration et al. (2020) that the formation of such

a high mass ratio system as an isolated binary is strongly suppressed in population synthesis simulations. This is certainly true at Milky-Way metallicity where stellar winds are much stronger and progenitors lose more mass throughout the binary evolution. This leads to lower maximum BH masses and subsequently limits the maximum-mass ratio for BBH as well as BH-NS systems (Kruckow et al. 2018). However, this already posed a challenge for previous detection of BBH with large total mass. It is assumed that these systems have to originate from a lower metallicity environment (see, e.g., Stevenson et al. 2017). Especially Kruckow et al. (2018) have shown that there is a significant population of BBH as well as BH-NS systems with low mass ratios at low metallicity which match the source of GW190814. Together with the broad range of resulting merger times the birth as an isolated binary constitutes still a viable formation channel, although it challenges current supernova explosion mechanisms (Zevin et al. 2020). Alternative formation scenarios might include the merger of quadruple systems (Hamers & Safarzadeh 2020) or circumbinary accretion in a highly asymmetric progenitor system (Safarzadeh & Loeb 2020). Both, BBH and BH-NS systems, with strong asymmetry

are nonetheless suppressed compared to equal mass BBH binaries of the same total mass, due to mass transfer during the binary evolution equalising the companion masses to less asymmetric configurations. Additional alternative channels through dynamical captures or hierarchical binary systems are presented in [The LIGO Scientific Collaboration et al. \(2020\)](#). While the formation rates through these processes are not well known, they all need dense stellar environments to work and the probability to form such a system is independent of the low mass companion being a BH or a NS in these cases. Assuming a mass gap between NSs and BHs at approximately $5M_{\odot}$, the progenitor of the secondary companion has to be a NS. For both possibilities of forming the system in isolation or through dynamical processes, accretion of significant amounts of matter onto the NS or gaining angular momentum afterwards is very unlikely. Either due to the fact that the primary companion is evolving faster and thus collapses to a BH before the NS is formed, or because formation in dense stellar systems is only significant in mass segregated regions for which the timescale is much larger than the stellar evolution up to formation of the compact object.

Combining these implications, we conclude that the NS companion has to be born already with an approximate mass of $2.59M_{\odot}$ which is above the upper limit for the maximum mass for a nonrotating NS, $2.33M_{\odot}$ ([Rezzolla et al. 2018](#); [Shibata et al. 2019](#)). Consequently, such a NS has to be supported by rotation against gravitational collapse for a significant time after its birth. Long-term electromagnetic spin-down might lead to its collapse to a BH if a significant fraction of the spin has been removed. Such a BH would then inherit its mass and spin from the NS.

For the rest of the paper, we will assume that the secondary in GW190814, hence, was either a rapidly rotating NS or a BH formed by the gravitational collapse of such with the same properties. Given the well constrained mass of the low mass companion, we are able to use the universal relations between maximum supportable mass M_{crit} and the ratio of the stars dimensionless spin to its maximum dimensionless spin at the mass shedding limit found by [Breu & Rezzolla \(2016\)](#) to find a new lower bound on the maximum mass M_{TOV} a nonrotating NS must be able to support. Such a constraint can help to constrain the equation of state (EOS) of nuclear matter at densities beyond the reach of earth-based experiments. Indeed, in the recent past a number of studies have used the multimessenger signal of the event GW170817 ([The LIGO Scientific Collaboration & The Virgo Collaboration 2017](#)) in order to derive astrophysical constraints and/or translate them into constraints on the EOS ([Margalit & Metzger 2017](#); [Bauswein et al. 2017](#); [Rezzolla et al. 2018](#); [Ruiz et al. 2018](#); [Annala et al. 2018](#); [Radice et al. 2018](#); [Most et al. 2018a](#); [De et al. 2018](#); [Abbott et al. 2018](#); [Montaña et al. 2019](#); [Raithel et al. 2018](#); [Tews et al. 2018](#); [Malik et al. 2018](#); [Koepfel et al. 2019](#); [Shibata et al. 2019](#)). This work falls in line with these studies by deriving a new lower limit on M_{TOV} . Additionally, we give a lower bound on the dimensionless spin for the secondary companion, using the upper maximum-mass constraints from the GW170817 event ([Rezzolla et al. 2018](#); [Shibata et al. 2019](#)).

2 RAPIDLY SPINNING NEUTRON STARS: THE BASIC PICTURE

A binary system of two compact objects can be described in terms of their masses m_1 and m_2 ($< m_1$) and corresponding dimensionless spins $\chi_1 = S_1/m_1^2$ and $\chi_2 = S_2/m_2^2$, where S_1 and S_2 are the spin angular momentum of the two compact objects. For simplicity, we will consider only the component of the spins aligned with the orbital angular momentum, which is usually extracted from gravitational wave observations ([The LIGO Scientific Collaboration et al. 2020](#)). The effective spin is defined as

$$\tilde{\chi} := \frac{m_1\chi_1 + m_2\chi_2}{m_2 + m_1} = \frac{\chi_1}{1+q} \left(1 + q \frac{\chi_2}{\chi_1}\right), \quad (1)$$

where $q := m_2/m_1 \leq 1$ is the mass ratio of the binary system.

If one of the objects in the system is a NS, its maximally allowed mass M_{crit} will depend on its spin χ_1 . In particular, for a nonrotating NS $m_1 < M_{\text{TOV}}$, where M_{TOV} is the maximum mass of a nonrotating NS. Observations of PSR J0348+0432 indicate that $M_{\text{TOV}} > 2.01^{+0.04}_{-0.04} M_{\odot}$ ([Antoniadis et al. 2013](#)), with a recent observation of PSR J0740+6620 indicating that $M_{\text{TOV}} > 2.14^{+0.10}_{-0.09} M_{\odot}$, although with this large uncertainty already at the $1-\sigma$ level ([Cromartie et al. 2020](#)). While the GW signal of GW170817 did not rule out EOSs consistent with nuclear constraints and small maximum masses, $M_{\text{TOV}} \simeq 2.0M_{\odot}$ ([Malik et al. 2019](#)), the constraints imposed by the electromagnetic counterparts of GW170817 ([Abbott et al. 2017](#); [The LIGO Scientific Collaboration et al. 2017](#)) have led to upper bounds on the maximum mass of $M_{\text{TOV}} \lesssim 2.3M_{\odot}$ (see, e.g., [Margalit & Metzger 2017](#); [Rezzolla et al. 2018](#); [Ruiz et al. 2018](#); [Shibata et al. 2019](#)), although this value could be higher in the less likely case that GW170817 did not result in a BH ([Ai et al. 2019](#)). We discuss the impact of the assumption of an upper maximum mass at the end of the paper.

If the NS is spinning, its maximum mass can be higher than M_{TOV} due to the additional rotational support against gravitational collapse to a BH. In particular, [Breu & Rezzolla \(2016\)](#) have found that the critical mass M_{crit} , that is, the mass of uniformly rotating NSs on the mass stability line, can be expressed in a (quasi-) universal relation through the dimensionless spin on the stability line χ_{crit} ([Friedman et al. 1988](#); [Takami et al. 2011](#)), and the maximum dimensionless spin at the mass shedding limit χ_{Kep} ¹

$$M_{\text{crit}}(\chi_{\text{crit}}, \chi_{\text{Kep}}, M_{\text{TOV}}) := M_{\text{TOV}} \left(1 + a_1 \left(\frac{\chi_{\text{crit}}}{\chi_{\text{Kep}}}\right)^2 + a_2 \left(\frac{\chi_{\text{crit}}}{\chi_{\text{Kep}}}\right)^4\right), \quad (2)$$

where $a_1 = 0.132$, $a_2 = 0.071$. This directly implies that the maximum mass for any uniformly rotating NS is limited by the spin at the mass-shedding limit, $\chi_{\text{crit}} = \chi_{\text{Kep}}$, where

$$M_{\text{max}} := M_{\text{crit}}(\chi_{\text{crit}} = \chi_{\text{Kep}}) = \xi_{\text{max}} M_{\text{TOV}}, \quad \xi_{\text{max}} = 1.203 \pm 0.022, \quad (3)$$

¹ Note that maximum mass supported through uniform rotation is not the end-point of neither the turning-point line ([Friedman et al. 1988](#)), nor of the neutral-stability line ([Takami et al. 2011](#)), and it is always larger than both of them (see, e.g., [Weih et al. 2018](#); [Bozzola et al. 2019](#), for details).

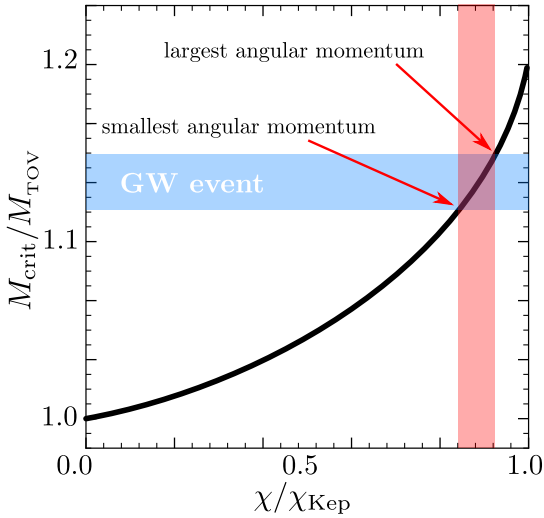


Figure 1. Schematic representation of the universal relation for uniformly rotating NSs along the stability line, (Breu & Rezzolla 2016). The solid black line reports the (quasi-)universal relation between $M_{\text{crit}}/M_{\text{TOV}}$ and the dimensionless angular momentum of the star when normalised to its maximum value χ/χ_{Kep} , while the blue-shaded area are the constraints on the mass from a given GW event. For any chosen M_{TOV} , the intersections of the blue-shaded area with the solid line will select the rotating stars having the smallest and the largest angular momentum.

as was shown in (Breu & Rezzolla 2016). Note that this result, combined with the present estimates on M_{TOV} implies a *strict* upper limit on the mass of a NS supported via uniform rotation, i.e., $M_{\text{max}} \leq 2.85 M_{\odot}$, which is clearly larger than the mass inferred for the secondary in GW190814.

Given a mass M_{crit} of a rapidly rotating NS it is possible to set bounds on its spin χ and the maximum mass M_{TOV} of a nonrotating NS. This is shown schematically in Fig. 1, which reports the universal relation for the masses of NSs along the stability line of uniformly rotating models M_{crit} (Breu & Rezzolla 2016). More specifically, the solid black line reports the (quasi-)universal relation between $M_{\text{crit}}/M_{\text{TOV}}$ and the dimensionless angular momentum of the star when normalised to its maximum value χ/χ_{Kep} , i.e., Eq. (2). One can see, for instance, that the largest possible mass for a rotating star M_{max} is ~ 1.2 times that of the corresponding nonrotating model for any EOS. Shown instead with a blue-shaded area are the constraints on the mass from a given GW event. This area will depend not only on the GW measurement, but also on M_{TOV} . The intersections of the blue-shaded area with the solid line will then select the rotating star on the stability limit having the smallest and the largest angular momentum that is still in agreement with the observation. The red-shaded area will therefore represent the allowed range in spin for a massive NS that has collapsed to a BH. Since $\chi \leq \chi_{\text{Kep}}$, it is also possible to determine a lower bound on M_{TOV} when $M_{\text{crit}} = M_{\text{max}}$, that is, when the lower limit of the observed mass range (lower edge of blue-shaded area) is reached by a star with $\chi = \chi_{\text{Kep}}$.

While the maximum mass M_{max} supported by a rapidly rotating NS does not depend on the numerical value of χ_{Kep} , it will turn out to be useful to give a more precise value that will be necessary to constrain the spin of the secondary in GW190814. Based on the results of Koliogiannis & Mous-

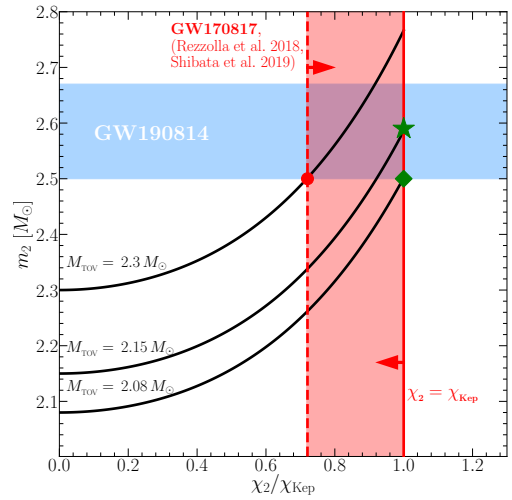


Figure 2. Mass over spin of the secondary in GW190814. The black lines show the Eq. (2) assuming that the secondary was a critically spinning NS at some point. The red-shaded area marks the allowed spin range given the mass measurement (blue shaded). The green diamond selects the curve with the minimal possible value of M_{TOV} , the green star the one corresponding to the most likely inferred mass of GW190814. We note that these constraints are independent of the actual value of χ_{Kep} .

takidis (2020), it is possible to express χ_{Kep} in terms of the compactness $C_{\text{TOV}} = M_{\text{TOV}}/R_{\text{TOV}}$, i.e., (Breu & Rezzolla 2016; Shao et al. 2020)

$$\chi_{\text{Kep}} \simeq \frac{\alpha_1}{\sqrt{C_{\text{TOV}}}} + \alpha_2 \sqrt{C_{\text{TOV}}}. \quad (4)$$

where $\alpha_1 = 0.045 \pm 0.021$ and $\alpha_2 = 1.112 \pm 0.072$ (Most et al. 2020). Using a large set of EOSs compatible with current bounds on the tidal deformability and constraints on the maximum mass of nonrotating NSs from GW170817 (Most et al. 2018a; Weih et al. 2019), it was possible to show that a lower/upper bound in compactness can be given in terms of M_{TOV} (Most et al. 2020), i.e.,

$$\sqrt{C_{\text{TOV}}^{\text{min}}} = c_1 M_{\text{TOV}} + c_2 M_{\text{TOV}}^2 + c_3 M_{\text{TOV}}^3, \quad (5)$$

$$\sqrt{C_{\text{TOV}}^{\text{max}}} = d_1 M_{\text{TOV}} + d_2 M_{\text{TOV}}^2 + d_3 M_{\text{TOV}}^3, \quad (6)$$

where $c_1 = 0.482$, $c_2 = -0.174$, $c_3 = 0.027$, $d_1 = 0.6522$, $d_2 = -0.256$, $d_3 = 0.034$.

3 APPLICATION TO GW190814

Recently the LIGO/Virgo collaboration has reported the detection of the merger of a $\sim 23 M_{\odot}$ BH with another $\sim 2.6 M_{\odot}$ compact object (The LIGO Scientific Collaboration et al. 2020). Following the scenarios outlined in Sec. 1 we assume that we have the merger of a very massive BH with a light BH that was produced by the collapse of a rapidly spinning NS prior to merger. We can then use the universal relations summarised in Sec. 2 to extract bounds on the spin χ_2 and m_2 of the secondary companion. Indeed, as we will comment later on, our bounds apply unchanged even if the rapidly spinning NS never collapsed to a BH.

In Fig. 2 we show the universal relation (2) of the mass m_2 of a rapidly spinning NS with its spin χ_2 . In addition, we also

shade the allowed region of masses of the secondary from the GW190814 event in blue (The LIGO Scientific Collaboration et al. 2020), i.e., $m_2 = 2.59^{+0.08}_{-0.08}$, and mark the maximally allowed spin $\chi_2 = \chi_{\text{Kep}}$ approximated as a constant with a red vertical line. Note that for different values for the maximum mass M_{TOV} , Eq. (2), generates a sequence of rotating stars starting at $m_2 = M_{\text{TOV}}$ and terminating at their maximum value when $\chi_2 = \chi_{\text{Kep}}$. If the secondary binary companion in GW190814 was at some point a NS (and since then did not change its mass significantly), it will have to lie on or below one of these sequences. As outlined in Sec. 2, the sequence with the lowest M_{TOV} that still intersects with the measurement of GW190814 marks (green diamond in Fig. 2) a lower limit on M_{TOV} , i.e., $M_{\text{TOV}}^{\text{min}}$. For the NS to have been stable initially, it could not have been more massive than the heaviest rotating configuration, i.e.,

$$m_2 \leq M_{\text{max}} \simeq \xi_{\text{max}} M_{\text{TOV}}^{\text{min}}, \quad (7)$$

where we have used Eq. (3). Hence, we find that if the secondary in GW190814 was either a BH formed by the collapse of a rapidly rotating NS or a stable rapidly rotating NS, this yields a lower bound on the maximum mass of nonrotating stars, i.e.,

$$M_{\text{TOV}} \gtrsim M_{\text{TOV}}^{\text{min}} = m_2^{\text{GW190814}} / \xi_{\text{max}} \approx 2.08 \pm 0.04 M_{\odot}, \quad (8)$$

where we have taken the most conservative lower limit on the companion mass $m_2^{\text{GW190814}} = 2.51 M_{\odot}$ (The LIGO Scientific Collaboration et al. 2020). For completeness, we also report the lower bound $M_{\text{TOV}}^{\text{opt}} \approx 2.15 \pm 0.04 M_{\odot}$ when using the most likely value of $m_2^{\text{opt}} = 2.59 M_{\odot}$. The corresponding sequence of critical masses of rotating NSs with spin χ_2 is given by the lower black line in Fig. 2, which terminates at $\chi_2 = \chi_{\text{Kep}}$. Two important remarks need to be made at this point as they are sometimes confused or misunderstood. First, M_{crit} depends only on M_{TOV} and not on the actual value of χ_{Kep} . This is because M_{crit} is deduced from universal relations expressed in terms of the normalised angular momentum χ/χ_{Kep} , de-facto removing any information on the precise (and EOS-dependent) value of χ_{Kep} . Hence, the lower maximum-mass bound in Eq. (8) is universal and agnostic of the EOS. Second, while the lower bound (8) is compatible with the measurement of Cromartie et al. (2020), the latter also has a rather large uncertainty, i.e., $2.14^{+0.10}_{-0.09}$ at $1 - \sigma$ and $2.14^{+0.20}_{-0.18}$ at $2 - \sigma$. Hence, the bound in Eq. (8) – whose derivation follows a completely different route – provides independent and complementary strength to the idea that NSs with masses $\gtrsim 2.1 M_{\odot}$ should be measured in the near future.

In accordance with the maximum-mass constraints described in Sec. 2, we can consider the same logic and draw lines for any value of $M_{\text{TOV}} \lesssim 2.3 M_{\odot}$, which is shown with different black lines in Fig. 2. From the intersection of the line corresponding to $M_{\text{TOV}} = 2.3 M_{\odot}$ with $m_2^{\text{GW190814}} = 2.51 M_{\odot}$ we deduce a lower bound of

$$\chi_2 / \chi_{\text{Kep}} \gtrsim 0.72. \quad (9)$$

In order to translate this constraint into an actual spin constraint, we need to fix the spin at break-up, χ_{Kep} . Using Eqs. (5) and (6) in Eq. (4) for χ_{Kep} , we find an average value of $\chi_{\text{Kep}} = 0.68$ for $2.01 \leq M_{\text{TOV}}/M_{\odot} \leq 2.3$, in accordance with those EOSs. This is consistent with an earlier

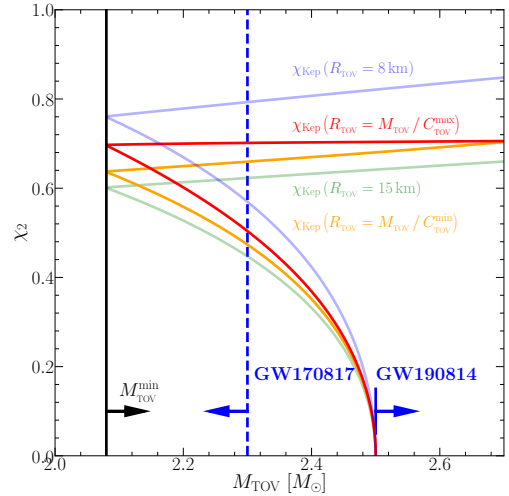


Figure 3. Dimensionless spin bounds for the secondary object. The upper (almost constant) lines refer to the Keplerian limit, which corresponds to the highest spin a uniformly rotating NS can attain. The lower curves correspond to the minimal amount of spin needed to support a $2.5 M_{\odot}$ star by means of (rapid) rotation. The various lines represent different values of χ_{Kep} as described in the figure and the text. The blue lines denote bounds from GW190814 and GW170817, respectively. The limiting spin configuration where the two lines intersect, will always happen at $M_{\text{TOV}}^{\text{min}}$ due to the universal relation between M_{max} and M_{TOV} .

constraint of $\chi_{\text{Kep}} \approx 0.7$ estimated from a small set of EOSs by Lo & Lin (2011). As we have pointed out in the derivation of Eq. (8), the lower bound $M_{\text{TOV}}^{\text{min}}$ on the maximum mass does not depend on $\chi_2 = \chi_{\text{Kep}}$, due to the separate universality of the maximum mass $M_{\text{crit}}(\chi_{\text{Kep}})$ only in terms of the M_{TOV} (see also the discussion around Eq. (2)). Thus, only the bounds on the spin χ_2 will explicitly depend on the precise value of χ_{Kep} via Eq. (4). For comparison we now adopt both the upper and lower bounds on C_{TOV} in terms of Eqs. (5) and (6), which are consistent with GW170817 (Most et al. 2020). In addition, we adopt very conservative ranges of $8 \leq R_{\text{TOV}}/\text{km} \leq 15$, in order to determine the most severe effect on the spin bound. The resulting spin bounds are shown in Fig. 3, which shows that the variations in the lower bound of the secondary’s spin are small and given by

$$0.49^{+0.08}_{-0.05} \lesssim \chi_2 \lesssim 0.68^{+0.11}_{-0.05}, \quad (10)$$

under the assumption that $M_{\text{TOV}} \leq 2.3 M_{\odot}$ (Rezzolla et al. 2018; Shibata et al. 2019). Stated differently, while it is useful to consider an uncertainty in the value of χ_{Kep} , the latter hardly affects our estimates (10) for the spin of the secondary in GW190814.

Finally, this range for χ_2 can be translated into a rotation frequency of the NS, $\Omega_2 = S_2/I_2$, that can be easily computed for a given moment of inertia I_2 , which can be expressed in terms of the NS mass and radius. Using the fit for $\chi \approx 0.4$ from Breu & Rezzolla (2016), we can compute the moment of inertia as

$$I_2/m_2^3 = \left(\bar{a}_1 C^{-1} + \bar{a}_2 C^{-2} + \bar{a}_3 C^{-3} + \bar{a}_4 C^{-4} \right), \quad (11)$$

with the compactness $C := m_2/R_2$ and $\bar{a}_1 = 9.50 \times 10^{-1}$, $\bar{a}_2 = 1.44 \times 10^{-2}$, $\bar{a}_3 = 1.22 \times 10^{-2}$, and $\bar{a}_4 = -7.61 \times 10^{-4}$. Assuming a typical NS radius of $R_2 = 12.5(13 \text{ km})$ (Most

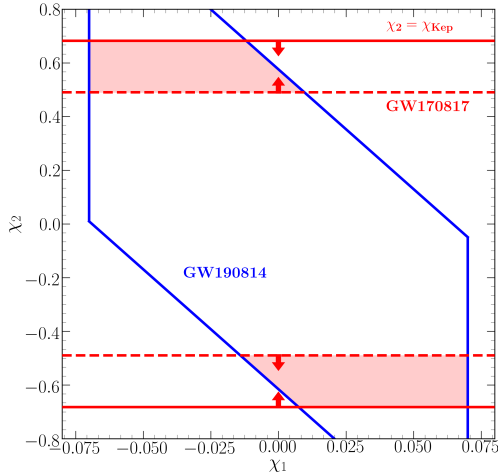


Figure 4. Allowed range (red-shaded area) of primary and secondary spins χ_1 and χ_2 , in case the secondary was a NS at some point before merger.

et al. 2018a) and $S_2 = \chi_2 m_2^2$, we find a rotation frequency $f = \Omega/2\pi$ of 1.21 (1.14) kHz for $\chi_2 = 0.49$. This frequency is considerably higher than the fastest known pulsar PSR J1748–2446ad (Hessels et al. 2006), with a frequency of 716 Hz, thus making – at least in this hypothetical scenario – the secondary of GW190814 the fastest known NS with a rotational kinetic energy $> 10^{52}$ erg. Assuming spins aligned/antialigned with the orbital angular momentum and using the fit given in Barausse & Rezzolla (2009) (see also Hofmann et al. 2016), we can derive an estimate on the final BHs spin, χ_{fin} . Assuming the spins of the primary and secondary are anti-aligned, we derive $0.24 < \chi_{\text{fin}} < 0.29$. Finally, we check the consistency of our estimates by computing the spin χ_1 of the primary via Eq. (1)

$$\chi_1(\chi_2) = -q\chi_2 + \tilde{\chi}(1+q), \quad (12)$$

and using $\tilde{\chi} = -0.002 \pm 0.06$ and $q = 0.112^{+0.008}_{-0.009}$ (The LIGO Scientific Collaboration et al. 2020). We find that the values obtained here are all consistent with those inferred by The LIGO Scientific Collaboration et al. (2020), i.e., $|\chi_1| < 0.07$. The overall allowed range of binary component spins is then shown in Fig. 4.

4 CONCLUSION

We have investigated how a lower bound on the maximum mass M_{TOV} of a nonrotating NS can be derived from the recent observation of the merger of a $\sim 2.6 M_{\odot}$ compact object with a $\sim 23 M_{\odot}$ BH (The LIGO Scientific Collaboration et al. 2020). More specifically, since the maximum-mass constraints from GW170817 (Margalit & Metzger 2017; Rezzolla et al. 2018; Ruiz et al. 2018; Shibata et al. 2019) and the observations of the very massive pulsars PSR J0348+0432 and PSR J0740+6620 (Antoniadis et al. 2013; Cromartie et al. 2020) indicate that the maximum mass of nonrotating NSs is lower than the measured mass of the secondary m_2 , rotation is needed to allow for the secondary compact object in GW190814 to have been a NS at some point in the inspiral. Using universal relations for the maximum mass of uniformly rotating NSs (Breu & Rezzolla 2016), we infer

a lower limit on the maximum mass of nonrotating NSs, $M_{\text{TOV}} > 2.08^{+0.04}_{-0.04} M_{\odot}$. The new lower limit on M_{TOV} does not exclude EOSs supporting massive nonrotating neutron stars, i.e., $M_{\text{TOV}} \gtrsim 2.5 M_{\odot}$, although the studies that have explored this scenario have indicated that M_{TOV} cannot be much higher than the existing observational limit (Fattoyev et al. 2020).

However, assuming the formation of a BH as the final remnant of GW170817, makes it difficult to reconcile such high maximum masses with the amount of angular momentum left after the merger and the ejected mass (see Gill et al. 2019; Shibata et al. 2019, for an extended discussion). Hence, imposing an upper limit $M_{\text{TOV}} \leq 2.3 M_{\odot}$ consistent with the multimessenger observation of GW170817 (Rezzolla et al. 2018; Shibata et al. 2019), restricts the amount of minimal spin of the secondary object to $0.49^{+0.08}_{-0.05} \lesssim \chi_2 \lesssim 0.68^{+0.11}_{-0.05}$, a quantity that has not been constrained by the observations of GW190814. Conversely, if the maximum mass was as high as $2.51 M_{\odot}$ (Ruiz et al. 2018), the spin required from Eq. (2) to support a $2.6 M_{\odot}$ NS, i.e., the average secondary mass in GW190814, would still be high, i.e., $\chi_2 > 0.31$. Even for this high estimate for the maximum mass, the rotation of the secondary can only be neglected, if the lower bound for the secondary mass, $m_2 > 2.51 M_{\odot}$, is assumed (Tsokaros et al. 2020), in agreement with the allowed spin parameter space delimited by the blue lines in Fig. 4.

Interestingly, since the rotational collapse of a magnetised NS to a BH can be accompanied by the emission of a radio signal similar to that measured in fast radio bursts (FRB) (Falcke & Rezzolla (2014) and also Most et al. (2018b)), there could be a potential connection between the location of an FRB and of a massive binary merger of the type discussed here.

ACKNOWLEDGEMENTS

It is a pleasure to thank R. Essick, P. Landry, M. Sarfarzadeh, and M. Zevin for useful discussions and comments. Support comes in part from HGS-HiRE for FAIR; the LOEWE-Program in HIC for FAIR; ‘‘PHAROS’’, COST Action CA16214; the ERC Synergy Grant ‘‘BlackHoleCam: Imaging the Event Horizon of Black Holes’’ (Grant No. 610058);

DATA AVAILABILITY

No new data was generated or analysed in support of this research.

REFERENCES

- Abbott B. P., et al., 2017, *Phys. Rev. Lett.*, **119**, 161101
Abbott B. P., et al., 2018, *Physical Review Letters*, **121**, 161101
Ai S., Gao H., Zhang B., 2019, arXiv e-prints, p. arXiv:1912.06369
Annala E., Gorda T., Kurkela A., Vuorinen A., 2018, *Phys. Rev. Lett.*, **120**, 172703
Antoniadis J., Freire P. C. C., Wex N., Tauris T. M., Lynch R. S., et al. 2013, *Science*, **340**, 448
Barausse E., Rezzolla L., 2009, *Astrophys. J. Lett.*, **704**, L40
Bauswein A., Just O., Janka H.-T., Stergioulas N., 2017, *Astrophys. J. Lett.*, **850**, L34
Bozzola G., Espino P. L., Davis Lewin C., Paschalidis V., 2019, arXiv e-prints, p. arXiv:1905.00028
Breu C., Rezzolla L., 2016, *Mon. Not. R. Astron. Soc.*, **459**, 646
Cromartie H. T., et al., 2020, *Nature Astronomy*, **4**, 72

- De S., Finstad D., Lattimer J. M., Brown D. A., Berger E., Biwer C. M., 2018, *Physical Review Letters*, **121**, 091102
- Falcke H., Rezzolla L., 2014, *Astron. Astrophys.*, **562**, A137
- Fattoyev F. J., Horowitz C. J., Piekarewicz J., Reed B., 2020, arXiv e-prints, p. [arXiv:2007.03799](https://arxiv.org/abs/2007.03799)
- Friedman J. L., Ipser J. R., Sorkin R. D., 1988, *Astrophys. J.*, **325**, 722
- Gill R., Nathanael A., Rezzolla L., 2019, *Astrophys. J.*, **876**, 139
- Hamers A. S., Safarzadeh M., 2020, *ApJ*, **898**, 99
- Hessels J. W., Ransom S. M., Stairs I. H., Freire P. C., Kaspi V. M., Camillo F., 2006, *Science*, **311**, 1901
- Hofmann F., Barausse E., Rezzolla L., 2016, *Astrophys. J. Lett.*, in press; arXiv:1605.01938,
- Koepfel S., Bovard L., Rezzolla L., 2019, *Astrophys. J. Lett.*, **872**, L16
- Koliogiannis P. S., Moustakidis C. C., 2020, *Phys. Rev. C*, **101**, 015805
- Kruckow M. U., Tauris T. M., Langer N., Kramer M., Izzard R. G., 2018, *Mon. Not. R. Astron. Soc.*, **481**, 1908
- Lo K.-W., Lin L.-M., 2011, *ApJ*, **728**, 12
- Malik T., Alam N., Fortin M., Providência C., Agrawal B. K., Jha T. K., Kumar B., Patra S. K., 2018, *Physical Review C*, **98**, 035804
- Malik T., Agrawal B. K., De J. N., Samaddar S. K., Providência C., Mondal C., Jha T. K., 2019, *Phys. Rev. C*, **99**, 052801
- Margalit B., Metzger B. D., 2017, *Astrophys. J. Lett.*, **850**, L19
- Montaña G., Tolós L., Hanauske M., Rezzolla L., 2019, *Phys. Rev. D*, **99**, 103009
- Most E. R., Weih L. R., Rezzolla L., Schaffner-Bielich J., 2018a, *Phys. Rev. Lett.*, **120**, 261103
- Most E. R., Nathanael A., Rezzolla L., 2018b, *Astrophys. J.*, **864**, 117
- Most E. R., Weih L. R., Rezzolla L., 2020, *Mon. Not. R. Astron. Soc.*, **496**, L16
- Radice D., Perego A., Zappa F., Bernuzzi S., 2018, *Astrophys. J. Lett.*, **852**, L29
- Raithe C., Özel F., Psaltis D., 2018, *Astrophys. J.*, **857**, L23
- Rezzolla L., Most E. R., Weih L. R., 2018, *Astrophys. J. Lett.*, **852**, L25
- Ruiz M., Shapiro S. L., Tsokaros A., 2018, *Phys. Rev. D*, **97**, 021501
- Safarzadeh M., Loeb A., 2020, arXiv e-prints, p. [arXiv:2007.00847](https://arxiv.org/abs/2007.00847)
- Shao D.-S., Tang S.-P., Sheng X., Jiang J.-L., Wang Y.-Z., Jin Z.-P., Fan Y.-Z., Wei D.-M., 2020, *Phys. Rev. D*, **101**, 063029
- Shibata M., Zhou E., Kiuchi K., Fujibayashi S., 2019, *Phys. Rev. D*, **100**, 023015
- Stevenson S., Vigna-Gómez A., Mandel I., Barrett J. W., Neijssel C. J., Perkins D., de Mink S. E., 2017, *Nature Communications*, **8**, 14906
- Takami K., Rezzolla L., Yoshida S., 2011, *Mon. Not. R. Astron. Soc.*, **416**, L1
- Tews I., Margueron J., Reddy S., 2018, *Physical Review C*, **98**, 045804
- The LIGO Scientific Collaboration The Virgo Collaboration 2017, *Phys. Rev. Lett.*, **119**, 161101
- The LIGO Scientific Collaboration the Virgo Collaboration 2020, arXiv e-prints, p. [arXiv:2004.08342](https://arxiv.org/abs/2004.08342)
- The LIGO Scientific Collaboration et al., 2017, *Astrophys. J. Lett.*, **848**, L12
- The LIGO Scientific Collaboration et al., 2020, arXiv e-prints, p. [arXiv:2006.12611](https://arxiv.org/abs/2006.12611)
- Tsokaros A., Ruiz M., Shapiro S. L., 2020, arXiv e-prints, p. [arXiv:2007.05526](https://arxiv.org/abs/2007.05526)
- Weih L. R., Most E. R., Rezzolla L., 2018, *Mon. Not. R. Astron. Soc.*, **473**, L126
- Weih L. R., Most E. R., Rezzolla L., 2019, *Astrophys. J.*, **881**, 73
- Zevin M., Spera M., Berry C. P. L., Kalogera V., 2020, arXiv e-prints, p. [arXiv:2006.14573](https://arxiv.org/abs/2006.14573)